The Journal of Experimental Biology 204, 1889–1899 (2001)
Printed in Great Britain © The Company of Biologists Limited 2001
JEB3479

DYNAMICS OF PAVEMENT CELL–CHLORIDE CELL INTERACTIONS DURING ABRUPT SALINITY CHANGE IN *FUNDULUS HETEROCLITUS*

K. DABORN, R. R. F. COZZI AND W. S. MARSHALL*

Biology Department, Saint Francis Xavier University, PO Box 5000, Antigonish, Nova Scotia, Canada B2G 2W5

*Author for correspondence (e-mail: bmarshal@stfx.ca)

Accepted 19 March 2001

Summary

Freshwater-adapted killifish (*Fundulus heteroclitus*) opercular epithelia were dissected and subjected to blood-side hypertonic bathing solution in Ussing-style chambers to simulate the increase in blood osmolality during migration to sea water. Conversely, seawater-acclimated killifish opercular epithelia were subjected to hypotonic bathing solutions to simulate the initial stages of migration to fresh water. Freshwater-acclimation (hypertonic stress) induced a rapid (approximately 30 min) increase in membrane conductance (G_t) from 3.10±0.56 to 7.52±1.15 mS cm^{-2} (P<0.01, N=27), whereas seawater-acclimation (hypotonic stress) induced a rapid decrease in G_t from 8.22±1.15 to 4.41±1.00 mS cm^{-2} (P<0.01, N=27; means ± S.E.M.). Control seawater-acclimated membranes had a density of apical crypts (where chloride cells are exposed to the environment; detected by scanning electron microscopy) of 1133±96.4 crypts mm^{-2} (N=12), whereas the hypotonically shocked specimens had a lower crypt density of 870±36.7 crypts mm^{-2} (P<0.01 N=10; means ± S.E.M.). Hypertonic shock of freshwater membranes increased crypt density from 383.3±73.9 (N=12) to 630±102.9 crypts mm^{-2} (P<0.05; N=11; means ± S.E.M.). There was no change in density of chloride cells, as detected by fluorescence microscopy; hence, osmotic stress changes the degree of exposure, not the number of chloride cells. Cytochalasin D (5.0 μmol l^{-1}) completely blocked the conductance response to hypotonic shock and the reduction in apical crypt density measured by scanning electron microscopy, while phalloidin (33 μmol l^{-1}), colchicine (3×10^{-4} mol l^{-1}) and griseofulvin (1.0 μmol l^{-1}) were ineffective. Actin imaging by phalloidin staining and confocal microscopy revealed extensive actin cords in pavement cell microridges and a ring of actin at the apex of chloride cells. We conclude that the actin cytoskeleton of chloride cells is required to maintain crypt opening and that osmotic shock causes chloride cells to adjust their apical crypt size.

Key words: opercular epithelium, killifish, salinity acclimation, ultrastructure, phalloidin, cytochalasin D, actin cytoskeleton, *Fundulus heteroclitus*.

Introduction

Freshwater teleosts have extracellular fluids that are hyperosmotic to their environment, and they constantly gain water osmotically and lose ions by diffusion. Teleosts generally lose ions passively through the permeable body surfaces such as the skin and gills (for reviews, see Perry, 1997; Karnaky, 1998). The mechanism for balancing the ion loss and osmotic water gain is the active uptake of ions across the gill and opercular surfaces and the production of hypotonic urine (Perry, 1997; Karnaky, 1998). The ion-uptake mechanism in rainbow trout is thought to be associated with acid–base regulation, wherein passive entry of Na^+ is driven by an electrochemical gradient generated locally by active transport of H^+ (Lin and Randall, 1993; for a review, see Perry, 1997). Freshwater-adapted killifish, however, seem not to conform closely to this model and instead display unusually low-affinity uptake mechanisms for Na^+ and Cl^- that may contribute to the rapid and powerful acclimation abilities of the species (Patrick et al., 1997).

Conversely, seawater-adapted killifish tend to lose water osmotically to the external environment and take up ions passively. Therefore, many marine teleosts will ingest the surrounding water, resorb salts and water across the intestine and secrete NaCl *via* mitochondria-rich (chloride) cells that are located in the gill and opercular epithelia (for reviews, see Wood and Marshall, 1994; Marshall, 1995; Marshall and Bryson, 1998). The currently accepted model for Cl^- secretion (Silva et al., 1977; Marshall and Bryson, 1998) is governed by the electrochemical gradient produced by the action of Na^+/K^+-ATPase, which is the active basolateral transport pump. A basolateral, bumetanide-sensitive $Na^+/K^+/2Cl^-$ cotransporter facilitates the uptake of Cl^- into the cell, where the Cl^- accumulates above its electrochemical equilibrium in the intracellular cytoplasm and exits following the electrochemical gradient through specific anion channels in the apical membrane that are similar to the cystic fibrosis transmembrane conductance regulator (CFTR; Marshall et al., 1995). Singer et

al. (Singer et al., 1998) cloned and sequenced killifish CFTR (kfCFTR) and demonstrated expression of the anion channel in *Xenopus laevis* oocytes. Secretion of Na^+ follows the generated electrochemical gradient through a cation-selective paracellular pathway between accessory and chloride cells (Sardet et al., 1979; Karnaky, 1991).

There are several studies reporting variations in chloride cells with salinity. Pisam et al. (Pisam et al., 1987) described the presence of two different types of chloride cell, an α and a β type, distinguished by the difference in the electron density, size and shape. The β-cells tended to be larger and more electron-dense (Pisam et al., 1987). Furthermore, during acclimation from fresh water to sea water, the β-cells disappear while the α-cells remain in both freshwater- and seawater-acclimated individuals. The functions of α- and β-cells are still undetermined. Several studies have examined the ultrastructure of the basolateral and apical surfaces of the mitochondria-rich chloride cells of gill and opercular epithelia. Marshall et al. (Marshall et al., 1997) used DASPEI fluorescence and scanning electron and transmission electron microscopy techniques to map the surface and subsurface structures of chloride cells both freshwater- and seawater-acclimated killifish. Hootman and Philpott (Hootman and Philpott, 1979) and Pisam and Rambourg (Pisam and Rambourg, 1991) described a tubular system that is continuous with the basolateral surface, and mitochondria-rich cells that contain Na^+/K^+-ATPase.

It has been demonstrated that in tilapia (*Oreochromis mossambicus*) the subcellular structure of the chloride cell changes during acclimation to sea water and, furthermore, that the basolateral tubule system increases in complexity during acclimation to sea water, accompanied by a marked increase in cell size (Foskett et al., 1981). The transition from fresh water to sea water also causes an increase in the number of Cl^--secreting cells in killifish (Marshall et al., 1997). Generally, the apical surface of seawater-acclimated fish opercular epithelium is pockmarked by apical crypts of varying size, each surrounded by flattened pavement cells. However, after acclimation to fresh water, these crypts were less apparent. The freshwater-adapted fish had chloride cells (as observed by scanning electron microscopy and transmission electron microscopy) that were covered over by pavement cells and, presumably, did not contribute to freshwater ion regulation (Marshall et al., 1997).

Chloride cell morphology and function in freshwater teleosts have been studied in depth (Laurent and Perry, 1991; Perry and Goss, 1994; Laurent et al., 1995). Acidification of water and hyperoxia (4 days) increase the fractional surface area of gill chloride cells without changing chloride cell density (Laurent and Perry, 1991), indicating morphological responses to environmental change. Metabolic alkalosis (HCO_3^- infusion) and cortisol treatment also increase the number and fractional surface area of exposed chloride cells in freshwater rainbow trout (Perry and Goss, 1994). Laurent et al. (Laurent et al., 1995) examined the Lake Magadi tilapia (*Oreochromis alkalicus grahami*), an animal uniquely adapted to severely alkaline fresh water. These tilapia possess well-developed gill chloride cells that have open apical crypts in water at pH 10, but the apical crypts close in water at pH 7 (2–3 h of treatment). The crypts reopen in response to long-term (24 h) treatment in water at pH 7, thus demonstrating the variability in apical membrane exposure. All the above changes were observed over periods of days, but there are two references to rapid morphological changes in chloride cells. There may be rapid alteration of tight junctions in chloride cells (Karnaky, 1991). Also, Sakamoto et al. (Sakamoto et al., 2000) observed rapid (within 30 min) reductions in exposure of chloride cells in mudskippers (*Periophthalmus modestus*) transferred to fresh water, an effect that was reversible on re-entry to sea water.

The present research aims to determine whether there is a regulation of ion transport on the basis of exposure or covering over of the apical crypts of chloride cells in response to osmotic shock because the cues and mechanisms that regulate the number and size of crypts are not yet known. An increase in basolateral osmolality markedly stimulates Cl^- secretion by the opercular epithelium of *Fundulus heteroclitus* (Zadunaisky et al., 1995) and is associated with natural increases in plasma osmolality on transfer to sea water (Marshall et al., 1999). Rapid serosal hypotonic shock decreases the short-circuit current (I_{sc}) and increases the membrane conductance (G_t), effects that reach a new steady state in 30–45 min (Marshall et al., 2000). Therefore, it can be hypothesized that changes in blood osmolality could affect the density of apical crypts. Furthermore, this study attempts to reveal an apparent sequence of events involving a cessation of ion secretion, a reduction in apical crypt density and passive ion loss on entry of euryhaline teleosts to fresh water (Wood and Marshall, 1994). To this end, the present study investigated the ultrastructural changes in the opercular epithelia associated with the acclimation of the euryhaline teleost *Fundulus heteroclitus* from sea water to fresh water and from fresh water to sea water. Electrophysiological observations were used to track any changes in the membrane potential (V_t), membrane conductance (G_t) and short-circuit current (I_{sc}), which is equivalent to the Cl^- secretion rate (Degnan et al., 1977; Marshall, 1981; Marshall and Nishioka, 1980). Scanning electron microscopy was used to examine the surface of the opercular epithelia, and dimethylaminostyrylethylpyridinium iodide (DASPEI) fluorescence microscopy was used after the experiments to estimate the density of mitochondria-rich cells. Finally, Oregon Green phalloidin staining of F-actin allowed the actin cytoskeleton in chloride cells and pavement cells to be examined. This work has appeared in part in abstract form (Daborn and Marshall, 1999).

Materials and methods

Animals

The specimens of *Fundulus heteroclitus* used for these experiments were collected from brackish, estuarine waters in Jimtown, Antigonish County, Nova Scotia, Canada, and were initially kept in 100 % sea water for 24 h, then transferred to

10 % sea water. Later, the specimens were acclimated to either fresh water or full-strength sea water (30 ‰). The fresh water had a composition (in mmol l^{-1}) of: 1.0 Na^+, 1.0 Cl^-, 0.02 Ca^{2+}, 0.06 Mg^{+2} and 0.02 K^+, with a pH of 6.8–7.2. The animals were held at room temperature (20–23 °C) and exposed to the natural, ambient photoperiod under artificial fluorescent light. The fish were fed marine fish food at a rate of 1 % body mass per day, supplemented twice weekly with freeze-dried tubifex worms (all food from Rolf C. Hagen, Montreal, Canada). The experiments were paired, with one control and one experimental membrane from each experimental animal.

Bathing solutions

The standard bathing solution used was a Cortland's saline (in mmol l^{-1}): NaCl, 159.9; KCl, 2.55; $CaCl_2$, 1.56; $MgSO_4$, 0.93; $NaHCO_3$, 17.85; NaH_2PO_4, 2.97; glucose, 5.55. This had a measured osmolality of 307 mosmol kg^{-1}. The saline was bubbled with a 99 % O_2/1 % CO_2 gas mixture prior to and during the experimentation. The resulting solution had a pH of 7.8 and was incubated at a temperature of 22 °C.

The hypotonic bathing solution used with the seawater-acclimated fish was composed of 75 % Cortland's saline diluted with 25 % distilled water. The resulting osmolality was 230 mosmol kg^{-1}. Basolateral hypotonicity produces rapid, reversible decreases in I_{sc} and G_t (Marshall et al., 2000).

For freshwater fish, the isotonic bathing solution was identical to the hypotonic bathing solution for seawater fish (osmolality of 230 mosmol kg^{-1}). The hypertonic bathing solution used with the freshwater fish was composed of the diluted Cortland's saline with 40 mmol l^{-1} of NaCl added. The resulting solution had a measured osmolality of 305 mosmol kg^{-1}. The solutions were changed three times with 10 ml flow-through of the Ussing-style chamber with the new bathing solution while the old solution was removed by suction.

Electrophysiology

Left and right opercular epithelia of each fish were dissected and mounted *in vitro* in Ussing-style membrane chambers (see Marshall et al., 1999) connected to a dual current/voltage-clamp apparatus (World Precision Instruments DVC-1000). The membranes were subjected to an initial control period of not less than 1 h during which the membrane conductance (G_t, mS cm^{-2}), the transepithelial potential (V_t, mV, mucosal side grounded) and the short-circuit current (I_{sc}, μA cm^{-2}, expressed as positive for anion secretion) were monitored. V_t was initially clamped to 0 mV to measure I_{sc}, then to +5.0 mV for a period of 1 s every 3 or 5 min to calculate epithelial conductance.

After the control period, in which a steady-state I_{sc} was established, the membrane potential was checked, and the bathing solution on the basolateral (serosal) side of the epithelium was changed to the appropriate test solution (either hypertonic or hypotonic Cortland's saline) to simulate blood osmolality changes during common estuarine salinity fluctuations. The seawater-acclimated fish had the basolateral side of the epithelium exposed to a hypotonic bathing solution to simulate the transition from sea water to fresh water, while the freshwater epithelia were exposed to basolateral hypertonic bathing solution to mimic transfer from fresh water to sea water. Each solution exchange involved three changes with 10 ml flow-through (7–10 times the chamber volume) of the new bathing solution into the Ussing-style chamber while the old bathing solution was removed by suction to maintain a constant fluid level. To provide a control for the disturbance caused by the mechanical exchange of bathing solutions, the control also had a similar exchange of an identical control (isotonic) solution.

Reported results are from membranes (control and test) at steady-state I_{sc}, approximately 45 min after hypotonic shock. The epithelia and inserts were removed as a whole and placed in vials containing the same bathing solution. The epithelia were fixed for electron microscopy or stained for fluorescence microscopy.

Cytoskeletal agents

Cytochalasin D, which disrupts actin polymerization (Cereijido et al., 1981), was dissolved in dimethylsulphoxide (DMSO) and added at a final concentration of 5.0 μmol l^{-1} to both sides for 1 h in five of the control and hypotonically shocked seawater membranes, which were then fixed for scanning electron microscopy. Colchicine (dissolved in ethanol and added to both sides of the membrane at a final concentration of 3×10^{-4} mol l^{-1}, 1 h) has been shown to promote microtubule disassembly (e.g. Maetz and Pic, 1976), griseofulvin (dissolved in DMSO and added at 1.0 μmol l^{-1}, 1 h) has been shown to disrupt microtubule formation (Mullins and Snyder, 1979) and phalloidin, which is known to stabilize F-actin filaments in the cytoskeleton (Maguire, 1998), was dissolved in ethanol, added at 33 μmol l^{-1} and incubated with samples for 3.0 h. Addition of equivalent vehicle concentrations of ethanol or DMSO were without effect on I_{sc}.

Fluorescence microscopy

At the end of the experimental period, the epithelia were stained using 1.0 μmol l^{-1} DASPEI for a period of 30 min. This is a vital dye that specifically stains mitochondria (Bereiter-Hahn, 1976) and thereby indicates the presence of mitochondria-rich cells for the determination of cell size and density (cells mm^{-2}). Following staining, the tissue was examined under epifluorescence microscopy using a Zeiss Photomicroscope III (excitation 485 nm, barrier filter of 520 nm). The protocol for counting the cells was to focus the microscope on a randomly selected area of the tissue and count the number of fluorescent cells in 10 fields of view (total area 0.2 mm^2).

Actin staining

Opercular epithelia were dissected without the dermal chromatophore layer, pinned to modeller's wax, incubated in 100 nmol l^{-1} (final concentration) Mitotracker Red (Molecular Probes, Eugene, OR, USA) in saline for 45 min and rinsed with Cortland's saline to remove excess. Tissues were then fixed in paraformaldehyde (250 mg plus 10 mg of glutaraldehyde in

5.0 ml of ice-cold Cortland's saline) for 15 min. Tissues were rinsed in Cortland's saline and permeabilized with 0.3 ml of Triton X-100 in 100 ml of Cortland's saline for 10 min. Oregon Green phalloidin (Molecular Probes, Eugene, OR, USA) was added to 132 nmol l^{-1} (final concentration) in Cortland's saline for 90–150 min. Tissues were rinsed three times with fresh Cortland's saline and wet-mounted for observation by confocal microscopy (excitation 488 nm; barrier 510 nm; Olympus FV300).

Scanning electron microscopy

Opercular epithelia were dissected, laid on top of a square sheet of modeler's wax and pinned flat using insect pins. The ice-cold primary fixative for freshwater-acclimated specimens (10 ml of 0.2 mol l^{-1} phosphate buffer, 1.5 ml of 25 % glutaraldehyde and 3.5 ml of distilled water) was left on the epithelia for 1 h on ice and for 2 h at room temperature followed by a phosphate-buffered rinse for 15 min. The initial rinse solution was removed, and the surface of the membrane was washed with the buffer solution to remove debris. To correct for osmolality, the distilled water was replaced with Cortland's saline for seawater-acclimated specimens. The secondary fixative for freshwater-acclimated specimens (3 ml of 5 % OsO_4, 2 ml of distilled water and 10 ml of 0.2 mol l^{-1} phosphate buffer) was placed on the tissue at room temperature for 1 h, and rinsed twice with distilled water for 15 min at room temperature. For seawater-acclimated specimens, the distilled water was replaced with filtered Cortland's saline. The tissue was dehydrated through an ethanol dehydration series (30, 50, 70, 80, 85, 90, 95 and 100 %) with each solution on the tissue for at least 15 min. The tissues were cut into small circles with a diameter of 0.4 cm, dried to critical point and sputter-coated.

Determination of apical crypt density by scanning electron microscopy was performed using a double-blind test to pick either a control or an experimental epithelium at random, place it in the scanning electron microscopy and, at 750× magnification, to select at random 15 locations on the membrane (that had no fixation artifacts such as cracks or debris). These locations were then examined at 3500× magnification, and the number of visible crypt openings was counted. The total area counted for each membrane was approximately 30 000 μm^2, and density is expressed as crypts mm^{-2}.

Statistical analyses

The data are expressed as means ± 1 S.E.M. The control and experimental periods were analyzed using paired or unpaired two-tailed *t*-tests where applicable. Linear regression was performed when analyzing conductance and crypt density.

Results

Electrophysiology

The decrease in V_t, I_{sc} and G_t of seawater membranes occurred quickly after application of basolateral hypotonicity, commencing within 5 min and coming to a new steady state within 30–45 min, as did the increase in I_{sc} and G_t in freshwater membranes exposed to hypertonic shock (Table 1). The decrease in I_{sc} in seawater membranes was large, approximately 96 $\mu A\,cm^{-2}$, while the increase in I_{sc} in freshwater membranes was modest, approximately 6 $\mu A\,cm^{-2}$. There was no significant change in V_t of freshwater membranes following hypertonic shock (Table 1).

Cytochalasin D electrophysiology

Cytochalasin-D-treated (5.0 μmol l^{-1}) membranes did not exhibit as large a decrease in G_t as was normally observed in a hypotonically treated membrane (49 % decrease in controls compared with 21 % decrease in cytochalasin-D-treated membranes; $P<0.05$, $N=12$; unpaired *t*-test; Table 2). The decrease in I_{sc} was the same in the cytochalasin-D-treated membranes (55 % decrease in controls compared with 56 % decrease in cytochalasin-D-treated membranes; Table 2).

Table 1. *A summary of the electrophysiological and microscopic data*

Acclimation	Treatment	V_t (mV)	G_t (ms cm^{-2})	I_{sc} ($\mu A\,cm^{-2}$)	Apical crypt density (crypts mm^{-2})	Chloride cell density (cells mm^{-2})
Sea water	Basolateral isotonic	17.21±4.2	8.22±1.15	138.2±8.13	1133±96.4 (12)	1533±102.7 (5)
	Basolateral hypotonic	11.15±3.24	4.41±1.00	42.61±3.89	870±36.7 (10)	1466±92.9 (5)
	Percentage change	–16.6	–46.4	–69.2	–23.2	–4
	Hypotonic *versus* isotonic	$P<0.05$	$P<0.01$	$P<0.05$	$P<0.01$	NS
Fresh water	Basolateral isotonic	1.83±4.05	3.10±0.56	4.82±1.83	383.3±73.9 (12)	1666±107.3 (5)
	Basolateral hypertonic	1.49±3.76	7.52±1.15	10.73±2.13	630±102.9 (11)	1566±72.4 (5)
	Percentage change	–19	+143	+123	+64	–6
	Hypertonic *versus* isotonic	NS	$P<0.01$	$P<0.05$	$P<0.05$	NS

For electrophysiological data, $N=27$; other sample sizes are in parentheses.

Isotonic *versus* hypotonic electrophysiological comparisons are by paired two-tailed *t*-tests. Cell densities are compared by unpaired two-tailed *t*-tests.

NS, not significant ($P>0.05$).

The data include membrane potential (V_t, mV), conductance (G_t, mS cm^{-2}), short-circuit current (I_{sc}, $\mu A\,cm^{-2}$), apical crypt density measured by scanning electron microscopy (crypts mm^{-2}) and chloride cell density measured by DASPEI fluorescence (cells mm^{-2}).

Steady-state values immediately before osmotic perturbation and after a new steady-state I_{sc} had been established are reported.

Table 2. *A summary of the electrophysiological data for cytochalasin-D-pretreated seawater-adapted membranes exposed to basolateral hypotonic shock*

Pharmaceutical	Treatment	V_t (mV)	G_t (ms cm^{-2})	I_{sc} (μA cm^{-2})	Apical crypt density (crypts mm^{-2})
Control[1]	Isotonic	23.9±1.29	9.95±0.81	233.3±23.0	1166±87.5 (5)
	Isotonic+DMSO	24.75±1.80	9.44±0.87	223.3±21.1	
	Basolateral hypotonicity	20.37±2.34	4.80±0.56	101.5±13.5	
	Percentage change	–18	–49	–55	
Cytochalasin D[2]	Isotonic	21.77±1.40	9.25±0.67	194.4±14.85	
	Isotonic+cytochalasin D	18.23±1.47	10.25±1.01	168.7±11.10	
	Basolateral hypotonicity	11.25±1.84	8.05±1.20	74.42±9.29	1033±105.3 (5)
	Percentage change	–38	–21	–56	
Control *versus* cytochalasin D[3]		P<0.01	P<0.05	NS	NS

[1]Control specimens, seawater-acclimated, N=12 for electrophysiological data; other sample sizes are in parentheses.
[2]Cytochalasin D, 5.0 μmol l^{-1} in DMSO, added to both sides of seawater-acclimated membranes; N=12.
[3]Control *versus* cytochalasin D after hypotonic shock, unpaired *t*-test, two-tailed.
The data include membrane potential (V_t, mV), conductance (G_t, mS cm^{-2}), short-circuit current (I_{sc}, μA cm^{-2}) and apical crypt density measured by scanning electron microscopy (crypts mm^{-2}).
NS, not significant (P>0.05, unpaired *t*-test, two-tailed).
DMSO, dimethylsulphoxide.

Cytochalasin-D-treated membranes before hypotonic shock had V_t and I_{sc} values that were not significantly different from the control (isotonic) values (Table 2).

Griseofulvin, phalloidin and colchicine electrophysiology

Colchicine-treated membranes underwent the same decrease in G_t and I_{sc} after basolateral hypotonic shock as untreated controls (Table 3). The final V_t, I_{sc} and G_t values of the colchicine-treated membranes (N=9) were not significantly different from those of the control (N=6) membranes (P>0.1, P>0.22 and P>0.5, respectively, unpaired *t*-test; Table 3). There was also no significant difference between the final V_t,

Table 3. *Electrophysiological results for colchicine-, griseofulvin- and phalloidin-pretreated membranes exposed to basolateral hypotonicity*

Pharmaceutical	Treatment	V_t (mV)	G_t (ms cm^{-2})	I_{sc} (μA cm^{-2})
Control[1]	Isotonic	17.08±1.49	10.11±0.77	164.6±8.60
	Basolateral hypotonicity	13.56±1.75	5.65±0.86	73.6±10.43
Colchicine[2]	Isotonic	15.32±1.98	10.70±1.06	159.8±22.57
	Basolateral hypotonicity	15.17±2.30	5.66±0.48	87.2±14.16
Control *versus* colchicine		NS	NS	NS
Griseofulvin[3]	Isotonic	16.53±1.41	9.83±0.62	165.8±22.57
	Basolateral hypotonicity	13.48±2.69	5.17±0.47	68.9±14.79
Control *versus* griseofulvin		NS	NS	NS
Phalloidin control[4]	Isotonic	20.18±2.47	10.13±2.48	200.7±41.2
	Basolateral hypotonicity	12.28±2.92	4.93±0.95	69.3±18.9
Phalloidin	Isotonic	17.35±3.02	13.05±1.76	214.3±34.4
	Basolateral hypotonicity	11.48±2.18	8.17±1.57	82.6±9.3
Phalloidin control *versus* phalloidin		NS	NS	NS

[1]Control specimens, seawater-acclimated N=6.
[2]Colchicine (3×10^{-4} μmol l^{-1})-treated specimens, seawater-acclimated, N=9.
[3]Griseofulvin (1.0 μmol l^{-1})-treated specimens, seawater-acclimated, N=6.
[4]Phalloidin (33 μmol l^{-1}, 3 h)-treated specimens, seawater-acclimated, N=6,
NS, not significant (P>0.05, unpaired *t*-test, two-tailed).
The data include membrane potential (V_t, mV), conductance (G_t, mS cm^{-2}) and short-circuit current (I_{sc}, μA cm^{-2}).

I_{sc} and G_t values exhibited by the griseofulvin-treated membranes and the control values (P>0.1, P>0.3 and P>0.25, respectively; N=6, unpaired t-test; Table 3). The phalloidin-treated membranes also showed marked decreases in V_t, G_t and I_{sc} after hypotonic shock (34 %, 37 % and 61 %, respectively), similar to those of control membranes (with decreases of 39 %, 51 % and 65 %; P>0.8, P>0.3, P>0.5, respectively, N=6, unpaired t-test; Table 3).

Hypotonic shock and scanning electron microscopy

The epithelia were examined by scanning electron microscopy with special attention to the appearance or disappearance of apical crypts according to the tonicity of the experimental bathing solutions. Exposure to hypotonic solutions decreased the number of apical crypts compared with the paired control membranes in isotonic bathing solution (compare Fig. 1 and Fig. 2; P<0.01; Table 1). The fully acclimated seawater fish that served as controls had a mean crypt density of 1133±96.4 crypts mm^{-2} of exposed opercular epithelium (N=12). However, the experimental opercular epithelia, those that were exposed to a hypotonic bathing solution, had a lower crypt density of 870±36.7 mm^{-2}, a decrease of 23 % (P<0.01, N=10, unpaired t-test; Table 1).

Freshwater opercular epithelia were examined using the same techniques and for the same types of changes in the number of apical crypts (Fig. 3, Fig. 4). The freshwater control membranes had a mean crypt density of 383.3±73.9 crypts mm^{-2} (N=12). The hypertonic, experimental membranes had a significantly higher apical crypt density, 630±102.9 crypts mm^{-2}, an increase of 64 % (P<0.05, N=11, unpaired t-test).

Chloride cell density

Freshwater control membranes had a mitochondria-rich chloride cell density measured by DASPEI fluorescence of 1666±107.3 cells mm^{-2} (N=5) that was not significantly different from that of the experimental hypertonically shocked freshwater membranes, which had a density of 1566±72.4 cells mm^{-2} (P>0.18, N=5, paired t-test; Table 1). The seawater-acclimated control membranes had a chloride cell density of 1533±102.7 cells mm^{-2} (N=5), and the experimental, hypotonically shocked seawater membranes had a similar cell density of 1466±92.9 cells mm^{-2} (P>0.28, N=5, paired t-test; Table 1).

Cytochalasin D structural effects

Fig. 5 is a scanning electron micrograph of a hypotonically

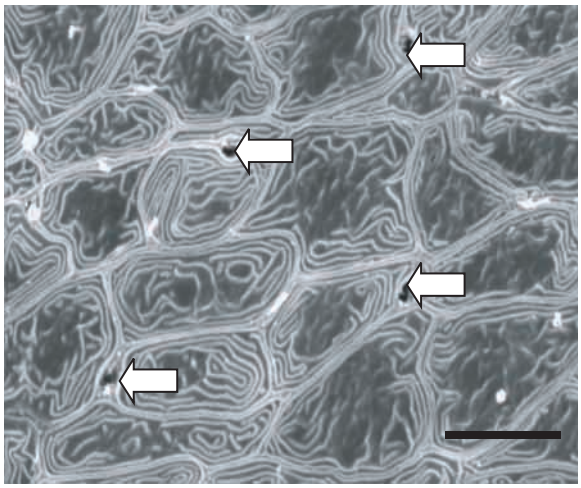

Fig. 2. Representative electron micrograph of the apical surface of the opercular epithelium of a fully acclimated seawater killifish subjected to a hypotonic shock on the basolateral surface for approximately 1 h. This opercular epithelium shows a considerably lower density of apical crypts (arrows) than the paired control (Fig. 1). Scale bar, 10 μm.

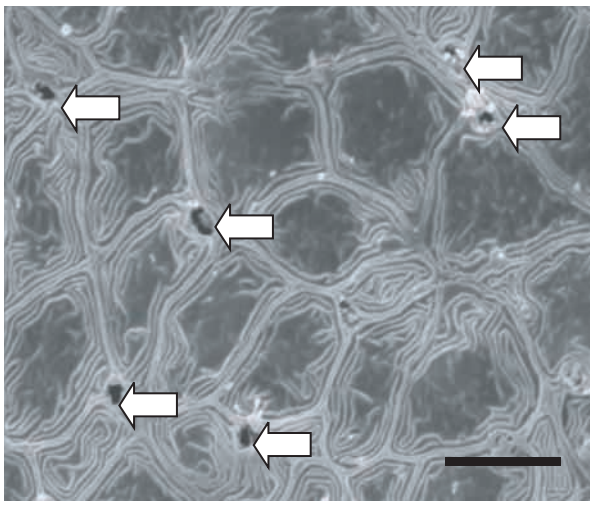

Fig. 1. Representative electron micrograph of the apical surface of a control opercular epithelium of a fully acclimated seawater killifish. Apical crypts (arrows) occur at high density. Scale bar, 10 μm.

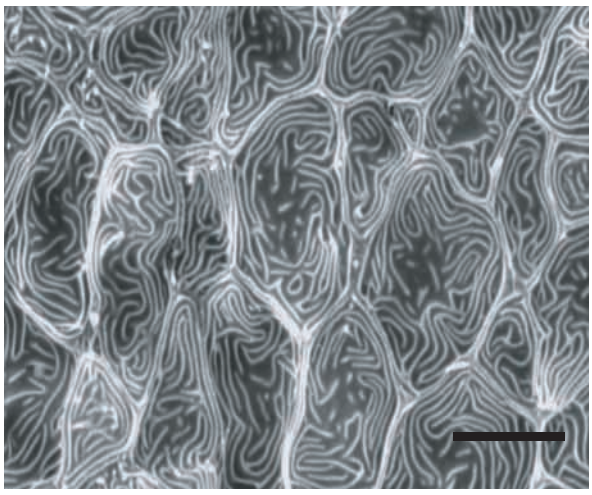

Fig. 3. Representative electron micrograph of the apical surface of a control opercular epithelium from a freshwater-acclimated specimen showing no apical crypts between the pavement cells. Scale bar, 10 μm.

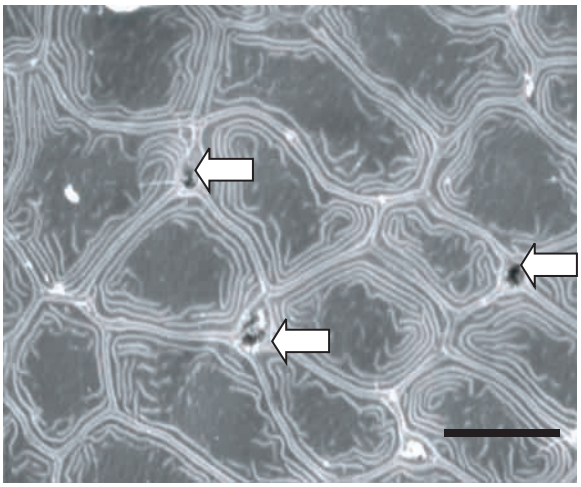

Fig. 4. Representative electron micrograph of a freshwater-acclimated killifish opercular epithelium treated with basolateral hypertonic shock. This epithelium shows a significantly higher density of apical crypts (arrows) than the freshwater control (Fig. 3). Scale bar, 10 μm.

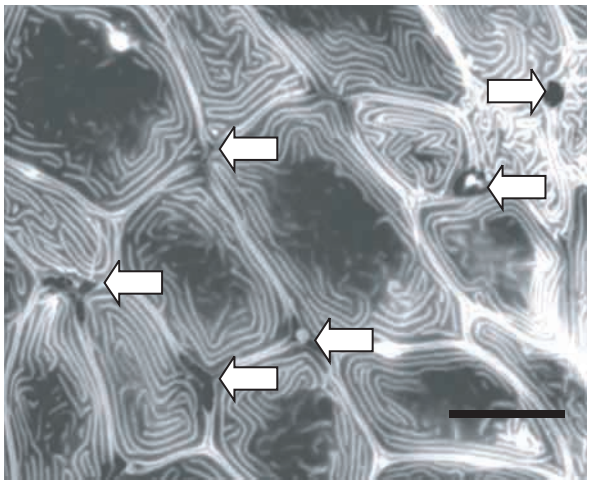

Fig. 5. Representative electron micrograph of a seawater-acclimated opercular epithelium pretreated with cytochalasin D, then treated with a hypotonic shock to the basolateral side. Note the failure of the apical crypts to close over and the high crypt density similar to that of seawater controls (Fig. 1). This micrograph also shows characteristic angular gaps between the cells (arrows). Scale bar, 10 μm.

shocked opercular epithelium from a seawater-acclimated killifish treated with cytochalasin D (5.0 μmol l^{-1}) on the serosal side. The density of apical crypts for the control (isotonically treated) membranes (N=5) was 1166.7±87.5 crypts mm^{-2}. The density of apical crypts for a cytochalasin-D-treated, hypotonically shocked (N=5) membrane was unchanged at 1033.33±105.3 crypts mm^{-2} (P>0.05, compared with isotonic controls, unpaired t-test, Table 2). The intercellular junctions between pavement cells, however, appeared to be weakened in cytochalasin-D-treated membranes because there were angular gaps between the microridge edges between adjacent pavement cells (Fig. 5).

Phalloidin staining of actin

Seawater opercular membranes were stained with phalloidin complexed with Oregon Green and observed by confocal fluorescence microscopy. Membranes that were not permeabilized had no specific staining even after 24 h of incubation. Permeabilized tissues stained well within 90–150 min and had the normal pattern of microridges seen previously by transmission electron microscopy and scanning electron microscopy (Fig. 6A,E) observed at the plane of the surface of the pavement cells. Whereas the junctions between pavement cells were double cords of actin (0.5–0.6 μm in diameter), around the lip of the apical crypts there was only a single cord of actin (0.25–0.3 μm in diameter) (Fig. 6A,C). Images taken 2.0 μm below the plane of the pavement cells revealed a well-developed thick (approximately 0.6 μm) actin ring at each apical crypt that we interpret as being the actin ring of the chloride cells (Fig. 6A,D). Images collected 6.0 μm deeper in the tissue reveal that Mitotracker-Red-positive chloride cells, often arranged in chloride cell and adjacent cell pairs, are situated directly below the actin rings of the apical crypts (Fig. 6B). Treatment of opercular membranes with cytochalasin D (same dose and time as for the electrophysiological experiments) produced progressive breakdown of the intercellular junctions between pavement cells (Fig. 6E), confirming that the phalloidin staining and the microridges seen by scanning and transmission electron microscopy are supported by an actin cytoskeleton. Longer incubation with cytochalasin D completely disrupted the junctions between pavement cells and resulted in these cells adopting a spherical rather than planar shape with sloughing of the epithelium (data not shown).

Conductance and scanning electron microscopy

The relationship between the spontaneous variation in the conductance of the opercular epithelia from freshwater animals *versus* the density of the apical crypts after hypotonic shock is shown in Fig. 7. As the density of the apical crypts decreases, the conductance of the membrane also decreases, leading to a hypothetical zero crypt density at a membrane conductance of 2.17±1.06 mS cm^{-2} (intercept ±95 % confidence interval) (r^2=0.7178, P<0.001). A similar regression of apical crypt density on the conductance for seawater membranes had the intercept 4.87±1.96 mS cm^{-2} (r^2=0.397, P<0.001), significantly higher than that for freshwater animals (regression not shown).

Discussion

The most important result of the present work is the finding that chloride cells may actively participate in the salinity acclimation process by closing or opening apical crypts in response to simple osmotic stimuli and that pavement cells close over and reduce ion permeability. In this way, there is a

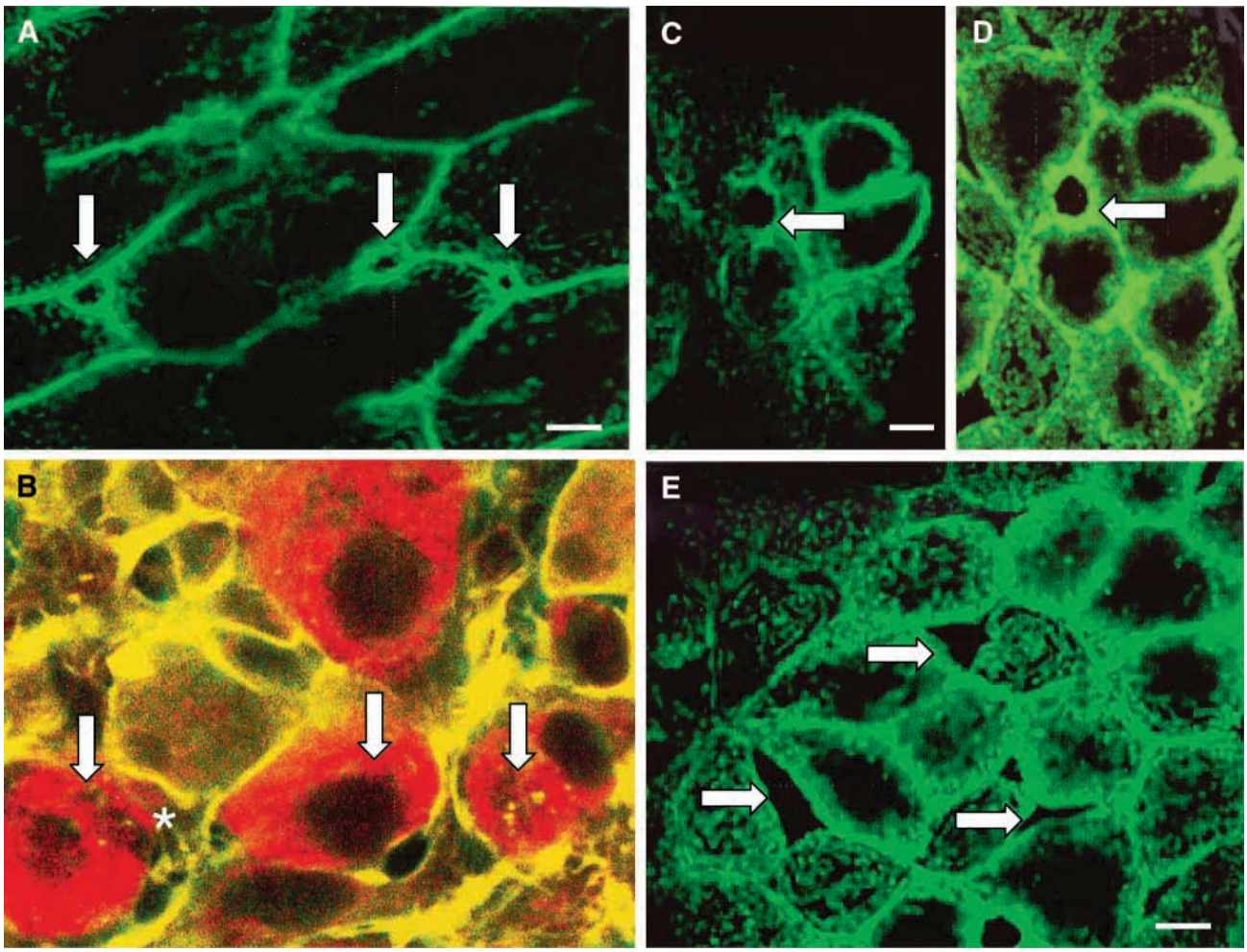

Fig. 6. Confocal microscope images of wet mounts of seawater-adapted killifish opercular epithelium. All are paraformaldehyde/glutaraldehyde-fixed, permeabilized and stained with Oregon Green phalloidin with or without Mitotracker Red pretreatment. (A) Fluorescence image of the opercular membrane at 1.5 μm below the plane of the pavement cells. Note the actin rings (arrows) of apical crypts. Scale bar, 5.0 μm. (B) The same frame as for A but 6.0 μm deeper into the tissue. Arrows are in the same locations and indicate apical crypts over mitochondria-rich chloride cells stained with Mitotracker Red. The asterisk indicates an adjacent cell. (C) Compare this image of opercular membrane fixed in paraformaldehyde with 0.1 % glutaraldehyde at the plane of the pavement cells with D, which shows the same frame but at a focal plane 2.0 μm below the plane of the pavement cells. Scale bar, 5.0 μm. Note the thick actin ring just below the opening of the apical crypt (arrow). (E) Opercular epithelium stained with Oregon Green phalloidin. The image was collected at the plane of the microridges of pavement cells. This tissue was pretreated with cytochalasin D and has typical angular gaps and holes between pavement cells (arrows), but the actin cords are for the most part intact. Scale bar, 5.0 μm.

potential for autoregulation at the tissue level of both passive and active ion-transport rates. Evidence for this interpretation comes from changes in apical crypt density, actin visualization and electrophysiological studies.

Apical crypt density and tonicity

The opercular membranes of seawater-acclimated *Fundulus heteroclitus* had a threefold greater density of apical crypts per square millimeter than the freshwater-acclimated fish (compare Fig. 1 and Fig. 3). This is consistent with the previously observed greater density of mitochondria-rich cells in fully acclimated animals (Marshall et al., 1997). The seawater-acclimated membranes had a lower density of crypts after a basolateral hypotonic shock (compare Fig. 1 and Fig. 2), but there was no change in chloride cell density (Table 1). The obvious explanation for the disappearance of apical crypts is that the crypts close and are covered over by pavement cells, providing an unbroken physical barrier to the diffusion of salts. Conversely, freshwater-acclimated membranes had a significantly increased crypt density when subjected to a hypertonic shock (compare Fig. 2 and Fig. 3; Table 1). The effect appears to be purely osmotic because reduction in [NaCl] at constant osmolality with added mannitol eliminates the reduction in I_{sc} and G_t normally seen with hypotonic shock (Marshall et al., 2000). Because these effects came to steady state after 45–60 min *in vitro*, it may be concluded that an early part of the salinity acclimation process includes the modification of apical crypt density and

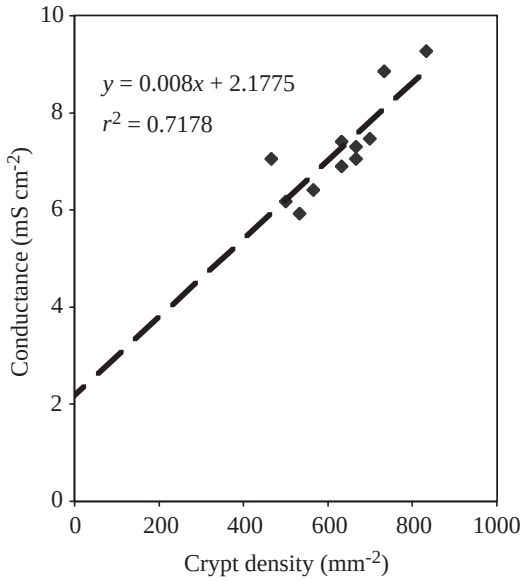

Fig. 7. Regression of the total epithelial conductance of the opercular epithelium on the density of apical crypts as detected by scanning electron microscopy for freshwater-acclimated animals (N=11). Epithelia have been exposed to basolateral hypertonicity. Extrapolation to the y-intercept gives an estimate of the conductance of an epithelium lacking apical crypt openings.

that the tissue can respond directly to changes in plasma (basolateral) osmolality.

Whereas it is well known that the opercular membranes of seawater-acclimated *Fundulus heteroclitus* have characteristic apical crypts (e.g. Philpott and Copeland, 1963) and there is a suggestion that apical tight junctions of chloride cells can change shape rapidly *in vitro* (Karnaky, 1991), the present work demonstrates how rapidly changes in apical crypt morphology occur as a result of osmotic stimuli. Previous observations of changes in the degree of exposure of chloride cells focused on acid–base disturbances over periods of days. Perry and Goss (Perry and Goss, 1994) suggested that increases in the fractional surface area of trout gill chloride cells (response to alkalization) could be the result of the retraction of pavement cells or the expansion of chloride cells. Here, we support the latter interpretation. Laurent et al. (Laurent et al., 1995) suggest that it was the pavement cell that initiated a closure of apical crypts in the chloride cells of Lake Magadi tilapia in response to reduced pH (from pH 10 to pH 7), but the apical crypts did not retain their (open) cup shape, rather the apex of the chloride cells appeared to narrow to less than 1.0 μm (Fig. 4 in Laurent et al., 1995) with the pavement cells joined over top. Mudskipper skin chloride cells react rapidly to salinity change in the whole animal and fewer chloride cells are exposed, as detected by concanavalin A/fluorescein staining of apical crypts (Sakamoto et al., 2000). Our work confirms the response and extends the conclusion by the use of scanning electron microscopy to detect apical crypts and offers an interpretation of the mechanism.

Cytoskeletal involvement

Pavement cells could swell osmotically with hypotonic shock to cover over apical crypts, but the response appears instead to be an active closure. The experiments with cytochalasin D showed that, by blocking the action of the actin cytoskeleton, the effect of hypotonic shock on apical crypt density is blocked. The density of apical crypts in a seawater-acclimated membrane treated with cytochalasin D and hypotonic shock was similar to that of seawater-acclimated membrane prior to hypotonic shock. Therefore, cytochalasin D blocks the closing of apical crypts by the actin cytoskeleton that normally follows hypotonic shock. In addition, the G_t of the hypotonically treated seawater membranes was significantly lower than the conductance for the cytochalasin-D- and hypotonic-shock-treated seawater-acclimated membranes; hence, cytochalasin D blocked the decrease in G_t normally seen with hypotonic shock. This supports the hypothesis that actin is involved in the conductance change and apical crypt closure. It also is consistent with previous work demonstrating that the conductance and ionic current of the membrane are localized to the apical crypts (Foskett and Scheffey, 1982). Finally, while the conductance change was clearly affected by cytoskeletal agents such as cytochalasin D (see above), the reduction in I_{sc} seen with hypotonic shock was unaffected by cytochalasin D or phalloidin, indicating that hypotonic effects on Cl^- secretion probably do not involve the actin cytoskeleton.

Griseofulvin and colchicine were ineffective at inhibiting the decrease in conductance. It would seem that microtubules, the cytoskeletal elements affected by griseofulvin and colchicine, are not involved in the response to the change in basolateral tonicity. Previous osmoregulatory effects obtained *in vivo* with systemic administration of colchicine (Maetz and Pic, 1976) probably have manifold contributory facets. Phalloidin was also without effect on the hypotonic response of living tissue, but our work with fluorescent derivative of phalloidin indicated that this agent does not penetrate the tissue well unless the cells have first been permeabilized.

There is evidence that the reduction in ion secretion precedes the closing over of crypts. Hypotonic shock immediately and dramatically decreases I_{sc}, and this change is complete before the G_t of the membrane comes to a new steady state (Fig. 2b in Marshall et al., 2000). Therefore, the active secretion of ions decreases before the crypts close. The continued decrease in G_t is consistent with the idea that apical crypts close over chloride cells that have already shut down ion secretion, rather than pavement cells actually effecting the shutdown by covering the apical crypts of secreting chloride cells.

Actin fluorescence

Oregon Green phalloidin staining of actin (Fig. 6) was most intense at the plane of the microridges of pavement cells. The fluorescence pattern was very similar in arrangement to the microridges typically seen in scanning electron micrographs of pavement cells, implying that the microridges are structurally supported by polymerized actin cords. This arrangement of the

microridges is consistent with previous transmission and scanning electron microscopy images (Sardet et al., 1979; Laurent et al., 1995; Marshall et al., 1997). Slightly below the plane of the pavement cells at the apical crypts is a thick ring of actin apparently in the chloride cell (Fig. 6A,C,D). This confirms the inference that chloride cells have a well-developed annular ring of actin. The circular shape of the rings formed by the apical crypt openings (seen by scanning electron microscopy and phalloidin fluorescence) suggests that the thicker chloride cell annular actin ring is structurally stronger than the thinner pavement cell actin and, hence, dominates the interaction between pavement and chloride cells. The actin rings of the apical crypts are located directly over mitochondria-rich chloride cell complexes, as detected by Mitotracker Red staining. Between pavement cells (with equal-thickness actin cords), the shape of the cell–cell interaction is always linear. Thus, it is likely that the chloride cell actively closes the apical crypt and that the pavement cells subsequently reseal over the crypt.

Conductance and crypt density

There is a proportional relationship between spontaneous variation in density of apical crypts and the conductance of the membrane (Fig. 7). This is consistent with the results of Sardet et al. (Sardet et al., 1979), who observed that the high permeability of the paracellular pathway in the seawater gill epithelium is associated with the leaky junctions between chloride cells and accessory cells and, therefore, should vary with the number of apical crypts. For seawater-acclimated control specimens, the number of apical crypts is very high (1133±96.4 crypts mm^{-2}), and the conductance is relatively high (8.22±1.15 mS cm^{-2}). In contrast, a control freshwater-acclimated specimen, with a very low crypt density (383.3±73.9 crypts mm^{-2}), has a much lower conductance (3.10±0.56 mS cm^{-2}). From the linear regression for freshwater controls, the total epithelial conductance varies directly with ionic permeability, in agreement with previous results (Karnaky and Kinter, 1977; Sardet et al., 1979; Marshall et al., 1997). In each case, the observed high density of apical crypts (in seawater-acclimated specimens) is associated with a high conductance of the membrane. Therefore, a hypotonic shock to a seawater-acclimated membrane decreases the number of apical crypts and the conductance, whereas a hypertonic shock to a freshwater-acclimated membrane evokes the opposite response.

By extrapolating the conductance of a tissue to zero crypt density, it is possible to estimate the conductance of a hypothetical tissue composed entirely of pavement cells. This was calculated to be 2.17±1.06 mS cm^{-2} (intercept ±95 % confidence interval; r^2=0.718; Fig. 7) using the freshwater membrane data that had the lowest density of crypts and was therefore closest to the hypothetical state (Fig. 7). The intercept is in close agreement with the 2.5 mS cm^{-2} observed by Wood and Pärt (Wood and Pärt, 1997), under similar conditions (with saline on both mucosal and serosal surfaces), for a cultured freshwater trout gill membrane that was shown by scanning electron microscopy to be a confluent pavement cell epithelium lacking chloride cells.

Actin and CFTR

The higher conductance per crypt in seawater membranes compared with freshwater membranes is appropriate if there is a change in the conductance of single chloride cells which, in turn, is consistent with the observed upregulation of the anion channel, a killifish homologue of human cystic fibrosis transmembrane conductance regulator (kfCFTR) (Marshall and Bryson, 1998; Singer et al., 1998) during seawater adaptation (Marshall et al., 1999). The apical location of actin in chloride cells is intriguing because this is also the apparent location of kfCFTR. Hypotonic shock of mammalian cells activates CFTR only in the presence of an active organized actin cytoskeleton (Prat et al., 1999). In killifish, hypotonicity instead decreases Cl^- transport rate (Marshall et al., 2000), but both systems are osmosensitive. Further, the CFTR channels in mammals and in killifish share activation by cyclic AMP *via* protein kinase A and have the same carboxy terminus, –DTRL, a ‘PDZ domain’. This terminal segment is suspected to be involved in trafficking of and actin protein binding to CFTR (for a review, see Kleizen et al., 2000); hence, the apical portions of chloride cells contain important components appropriate for actin-mediated trafficking of CFTR anion channels.

We thank the staff of the Animal Care Facility at Saint Francis Xavier University for their excellent care of the animals, Sharon Bryson for her support, John W. Mills for productive discussions and the NSERC and NS Department of Education NS Links Program for financial support. The work is in part the Honours BSc project of K.D.

References

Bereiter-Hahn, J. (1976). Dimethylaminostyrylmethylpyridinum iodide (DASPMI) as a fluorescent probe for mitochondria *in situ*. *Biochem. Biophys Acta* **423**, 1–14.

Cereijido, M., Meza, I. and Martinez-Palomo, A. (1981). Occluding junctions in cultured epithelial monolayers. *Am. J. Physiol.* **240**, C96–C102.

Daborn, K. and Marshall, W. S. (1999). Pavement cell–chloride cell interactions during abrupt salinity transfer in the estuarine teleost *Fundulus heteroclitus*: The peek-a-boo hypothesis. *Comp. Biochem. Physiol.* **124**A (abstract), S136.

Degnan, K. J., Karnaky, K. J. and Zadunaisky, J. A. (1977). Active chloride transport in the *in vitro* opercular skin of a teleost (*Fundulus heteroclitus*), a gill-like epithelium rich in chloride cells. *J. Physiol., Lond.* **271**, 155–191.

Foskett, J. K., Logsdon, C., Turner, T., Machen, T. and Bern, H. A. (1981). Differentiation of the chloride extrusion mechanism during seawater adaptation of a teleost fish, the cichlid *Sartherodon mossambicus*. *J. Exp. Biol.* **93**, 209–224.

Foskett, J. K. and Scheffey, C. (1982). The chloride cell: definitive indentification as the salt-secretory cell in teleosts. *Science* **215**, 164–166.

Hootman, S. R. and Philpott, C. W. (1979). Ultracytochemical localization of Na^+,K^+-activated ATPase in chloride cells from the gill of a euryhaline teleost. *Anat. Rev.* **193**, 99–130.

Karnaky, K. J., Jr (1991). Teleost osmoregulation: Changes in the tight junction in response to the salinity of the environment. In *The Tight Junction* (ed. M. Cereijido), pp. 175–185. Boca Raton, FL: CRC Press.

Karnaky, K. J. (1998). Osmotic and ionic regulation. In *The Physiology of Fishes*, second edition (ed. D. H. Evans), pp. 157–176. Boca Raton, FL: CRC Press.

Karnaky, K. J. and Kinter, W. B. (1977). Killifish opercular skin: A flat epithelia with a high density of chloride cells. *J. Exp. Zool*. **199**, 355–364.

Kleizen, B., Braakman, I. and De Jonge, H. R. (2000). Regulated trafficking of the CFTR chloride channel. *Eur. J. Physiol* **79**, 544–556.

Laurent, P., Maina, J. N., Bergman, H. L., Narahara, A., Walsh, P. J. and Wood, C. M. (1995). Gill structure of a fish from an alkaline lake: effect of short-term exposure to neutral conditions. *Can. J. Zool*. **73**, 1170–1181.

Laurent, P. and Perry, S. F. (1991). Environmental effects on gill morphology. *Physiol. Zool*. **64**, 4–25.

Lin, H. and Randall, D. J. (1993). H^+-ATPase activity in crude homogenates of fish gill tissue: inhibitor sensitivity and environmental and hormonal regulation. *J. Exp. Biol*. **180**, 163–174.

Maetz, J. and Pic, P. (1976). Microtubules in the 'chloride cell' of the gill and disruptive effects of colchicine on the salt balance of the seawater-adapted *Mugil capito*. *J. Exp. Zool*. **199**, 325–338.

Maguire, G. (1998). Actin cytoskeleton regulates ion-channel activity in retinal neurons. *Neuroreport* **19**, 665–670.

Marshall, W. S. (1981). Sodium dependency of active chloride transport across isolated fish skin (*Gillichthys mirabilis*). *J. Physiol., Lond*. **319**, 165–178.

Marshall, W. S. (1995). Transport processes in isolated teleost epithelia: Opercular epithelium and urinary bladder. In *Cellular and Molecular Approaches to Fish Ionic Regulation* (ed. C. M. Wood and T. J. Shuttleworth), pp. 1–23. New York: Academic Press.

Marshall, W. S. and Bryson, S. E. (1998). Transport mechanisms of seawater teleost chloride cells, an inclusive model of a multifunctional cell. *Comp. Biochem. Physiol*. **119**A, 97–106.

Marshall, W. S., Bryson, S. E., Darling, P., Whitten, C., Patrick, M., Wilkie, M., Wood C. M. and Buckland-Nicks, J. (1997). NaCl transport and ultrastructure of opercular epithelium from a freshwater adapted euryhaline teleost, *Fundulus heteroclitus*. *J. Exp. Zool.* **277**, 23–37.

Marshall, W. S., Bryson, S. E. and Luby, T. (2000). Control of epithelial Cl^- secretion by basolateral osmolality in the euryhaline teleost *Fundulus heteroclitus*. *J. Exp. Biol*. **203**, 1897–1905.

Marshall, W. S., Bryson, S. E., Midelfart, A. and Hamilton, W. F. (1995). Low conductance anion channel activated by cyclic AMP in teleost Cl-secreting cells. *Am. J. Physiol.* **268**, R963–R969.

Marshall, W. S., Emberly, T. R., Singer, T. D., Bryson, S. E. and McCormick, S. D. (1999). Time course of salinity adaptation in a strongly euryhaline estuarine teleost, *Fundulus heteroclitus*: a multivariable approach. *J. Exp. Biol*. **202**, 1535–1544.

Marshall, W. S. and Nishioka, R. S. (1980). Relation of mitochondria-rich chloride cells to active chloride transport in the skin of a marine teleost. *J. Exp. Zool.* **214**, 147–156.

Mullins, J. M. and Snyder, J. A. (1979). Effects of griseofulvin on mitosis in PtK1 cells. *Chromosoma* **72**, 105–113.

Patrick, M. L., Pärt, P., Marshall, W. S. and Wood, C. M. (1997). Characteristics of ion and acid–base transport in the freshwater adapted mummichog (*Fundulus heteroclitus*). *J. Exp. Zool*. **279**, 208–219.

Perry, S. F. (1997). The chloride cell: Structure and function in the gills of freshwater fishes. *Annu. Rev. Physiol*. **59**, 325–347.

Perry, S. F. and Goss, G. G. (1994). The effects of experimentally altered gill chloride cell surface area on acid–base regulation in rainbow trout during metabolic alkalosis. *J. Comp. Physiol*. B **164**, 327–336.

Philpott, C. W. and Copeland, D. E. (1963). Fine structure of chloride cells from three species of *Fundulus*. *J. Cell Biol*. **18**, 389–401.

Pisam, M., Caroff, A. and Rambourg, A. (1987). Two types of chloride cells in the gill epithelium of a freshwater adapted euryhaline fish: *Lebistes reticulatus*; their modifications during adaptation to saltwater. *Am. J. Anat*. **179**, 40–50.

Pisam, M. and Rambourg, A. (1991). Mitochondria-rich cells in the gill epithelium of teleost fishes: An ultrastructural approach. *Int. Rev. Cytol*. **130**, 191–232.

Prat, A. G., Cunningham, C. C., Jackson, G. R., Jr Borkan, S. C., Wang, Y., Ausiello, D. A. and Canniello, H. F. (1999). Actin filament organization is required for proper cAMP-dependent activation of CFTR. *Am. J. Physiol*. **277**, C1160–C1169.

Sakamoto, T., Yokota, S. and Ando, M. (2000). Rapid morphological oscillation of mitochondrion rich cell in estuarine mudskipper following salinity changes. *J. Exp. Zool.* **286**, 666–669.

Sardet, C., Pisam, M. and Maetz, J. (1979). The surface epithelium of teleostean fish gills, cellular and junctional adaptations of the chloride cell in relation to salt adaptation. *J. Cell Biol*. **80**, 96–117.

Silva, P., Solomon, R., Spokes, K. and Epstein, F. H. (1977). Ouabain inhibition of gill Na–K–ATPase: Relationship to active chloride transport. *J. Exp. Zool*. **199**, 419–426.

Singer, T. D., Tucker, S. J., Marshall, W. S. and Higgins, C. F. (1998). A divergent CFTR homologue: highly regulated salt transport in the euryhaline teleost *F. heteroclitus*. *Am. J. Physiol.* **274**, C715–C723.

Wood, C. M. and Marshall, W. S. (1994). Ion balance, acid–base regulation and chloride cell function in the common killifish, *Fundulus heteroclitus* – A euryhaline estuarine teleost. *Estuaries* **17**, 34–52.

Wood. C. M. and Pärt, P. (1997). Cultured branchial epithelia from freshwater fish gills. *J. Exp. Biol.* **200**, 1047–1059.

Zadunaisky, J. A., Cardona, S., Au, L., Roberts, D. M., Fisher, E., Lowenstein, B., Cragoe, E. J., Jr and Spring, K. R. (1995). Chloride transport activation by plasma osmolarity during rapid adaptation to high salinity of *Fundulus heteroclitus*. *J. Membr. Biol*. **143**, 207–217.